Lattice Discrete Particle Modeling of Time Dependent Behavior of Prestressed Concrete Beams.

Authors

Mohammed Abdellatef

PhD Graduate Student and research assistant, Department of Civil and Environmental Engineering, Rensselaer Polytechnic Institute, Troy, NY, USA; abdelm4@rpi.com

Jan Vorel

Christian Doppler Laboratory, University of Natural Resources and Life Sciences Vienna, Vienna, Austria; jan.vorel@fsv.cvut.cz

Roman Wendner

Director Christian Doppler Laboratory, University of Natural Resources and Life Sciences, Vienna, Austria, roman.wendner@boku.ac.at

Mohammed Alnaggar

Assistant Professor, Department of Civil and Environmental Engineering, Rensselaer Polytechnic Institute, Troy, NY, USA; alnagm2@rpi.edu

Abstract

Time dependent behavior of prestressed concrete (PC) structures is an essential factor in defining their serviceability limit states. Excessive creep and shrinkage deformations pose structural serviceability problems such as the 1.5 m beyond design camber that occurred in Koror-Babeldaob Bridge in 1996. With the current trend of using advanced cementitious materials to produce higher strength concretes, these long-term effects (including self desiccation) become more evident.

In this paper, coupled creep, shrinkage and aging evolution in prestressed concrete beams is simulated using a recently developed Discrete-Solidification-Microprestress (DSM)

formulation within the Lattice Discrete Particle Model (LDPM). Spatial and temporal evolutions of temperature, humidity and cementitious materials hydration are simulated using a Hygro-Thermo-Chemical (HTC) model. SDMP, DSM and LDPM are coupled in one framework to capture the interplay between environmental changes, creep and shrinkage deformation and damage. The formulations can capture early age as well as multi-decade creep and shrinkage deformations relevant to different design stages of prestressed/post tensioned concrete beams. Tendons are modeled using 1D finite element with a relaxation formulation that could be bound to concrete using a bond-slip type formulation.

Calibration and validation is performed through the simulation of multiple experimental data sets from literature.

Introduction

Time dependent deformations, such as creep and shrinkage, are considered major factors while design for serviceability limits of concrete structures. These deformations have more impact on prestressed concrete structures, as they could cause excessive deformations and loss of prestressing forces. An example for that is Koror-Babeldaob Bridge [1], where camber exceeded design limit of 1.5 meters. Although the bridge was retrofitted, it ended up collapsing few months later.

Several experimental programs studied long-term behavior of prestressed concrete structures, covering creep and shrinkage deformations [2,3] and relaxation [4]. These studies provided the needed database for design codes and numerical modeling developments.

In parallel, several finite element models were used to simulate and predict instantaneous and long-term behavior of prestressed concrete structures [5,6,7]. The main disadvantage of these models is the lack of concrete heterogeneity representation. Thus, discrete models are needed to better model and predict the complex short and long behavior of prestressed concrete structures.

In this paper, a multi-physics framework is used to model long-term behavior of post tensioned concrete beams under its own weight or sustained load. The discrete model

used is Lattice Discrete Particle Model (LDPM) [8,9] that is used to replicate elastic and damage behavior of concrete at the meso-scale (large aggregate pieces interaction scale) Visco-elastic and viscous deformations are modeled using a recently developed Discrete-Solidification-Microprestress (DSM)[10] formulation that was based on the Solidification-Microprestress Model by [11,12,13], to model the time dependency of strains with loading and environmental conditions. The comprehensive creep/shrinkage formulations are informed by a Hygro-Thermo-Chemical (HTC) Model [14] that evolves temperature, humidity, and cementitious materials hydration degree over both space and time. Thus, point-wise analysis of the structural elements is accurately performed accounting for the variations in environmental conditions and material aging. Steel relaxation was accounted for using the Eurocode 2 model [15].

Mechanical behavior

The mechanical behavior of concrete undergoing creep and shrinkage deformations was simulated by expressing each deformation component as an eigen-strain, which is imposed on the concrete meso-structure. The constitutive behavior of concrete is modeled using the Lattice Discrete Particle Model (LDPM). In the same discrete setting for the LDPM framework, assuming strain superposition to be valid throughout the procedure, one can rewrite in rate form, the total strain rate vector as a sum of the individual strain rates vectors from different phenomena involved as follows:

(1)

where represents the elastic, damage and cracking strain rates computed LDPM, and are shrinkage and thermal strain rates respectively, is the viscoelastic strain rate and is the purely viscous strain rate representing in sum, the creep strain rate and formulated based on the Micro-Prestress Solidification theory. Eq. (1) can be interpreted as the rheological model shown in figure 1a.

The prestressing forces are also imposed as eign-stain, acting on one-dimensional elements with both translational and rotational degrees of freedom, representing steel strands. The constitutive behavior of steel is assumed to be bilinear elasto-plastic model,

which allow evaluating imposed strains under a certain level of stress. An exponential relaxation model was also adopted from Eurocode 2, in order to account for time dependents relaxation losses of prestressing forces.

<Subhead 1>

The Lattice Discrete Particle Model (LDPM)

The Lattice Discrete Particle Model (LDPM) [8,9] is a meso-scale discrete model that simulates the mechanical interaction of coarse aggregate pieces embedded in a cementitious matrix (mortar). The concrete mesostructure is geometrically represented through a system of polyhedral cells (see figure 1b) interacting through triangular facets and a lattice system composed by the line segments connecting the particle centers. In LDPM, rigid body kinematics is used to describe the deformation of the lattice/particle system and the displacement jump , at the centroid of each facet is used to define measures of strain as:

(2)

Where = interparticle distance; and n, **l**, and m, are unit vectors defining a local system of reference attached to each facet. Next, a vectorial constitutive law governing the behavior of the material is imposed at the centroid of each facet. In the elastic regime, the normal and shear stresses are proportional to the corresponding strains:

(3)

Where , , = effective normal modulus, and α is shear-normal coupling parameter; and , , are mesoscale eigenstrains that might arise from a variety of phenomena such as, but not

limited to, thermal expansion, shrinkage, corrosion, Sulfate attack and ASR expansion.

For constitutive relations of stresses and strains beyond the elastic limit, one can refer to [8]. LDPM has been used successfully to simulate concrete behavior under a large variety of loading conditions. Furthermore it was successfully used to: account for fiber reinforcement [16], simulate the ballistic behavior of ultra-high performance concrete (UHPC) [17], simulate Alkali-Silica Reaction (ASR) deterioration [18] and nondestructive evaluation [19], reinforced concrete flexural and shear behavior [20], creep and shrinkage concrete behavior [10], and corrosion and rebar pullout [21]. In addition, LDPM was successfully used in structural element scale analysis using multiscale methods [22,23].

<Subhead 1>

Thermal and hygral deformations

Thermal and hygral variation effects on concrete skeleton are treated as eigenstrains inducing only volumetric deformations (no shear deformations), assuming that they only change the material physical state. For the range of application of the current model which is only below boiling temperature and above freezing temperature for water, the thermal and shrinkage strain rates respectively are and , where are is a constant coefficient of thermal expansion and is a constant shrinkage coefficient.

<Subhead 1>

Discrete-Solidification-Microprestress (DSM) for viscous and visco-elastic deformations

According to the Microprestress Solidification (MS) Theory [11], the viscoelastic behavior of concrete is modeled through the sum of three components. Following the original formulation of the MS theory, all the macroscopic components were reformulated at the meso-scale and equivalent parameters were used [10]. The first is the instantaneous strain rate corresponding to the elastic deformations induced by instantaneous change of stress . It is modeled by defining an instantaneous elastic modulus of concrete as , where is an age independent model parameter. LDPM elastic behavior is used to simulate this

behavior by redefining the mesoscale elastic modulus as , where (in) is a mesoscale model parameter that corresponds to in the original formulation. When all stresses are within their elastic limits, this formulation gives .

The second component is viscoelastic strain rate, which is formulated as , where and represents the cement gel visco-elastic micro strain rate, is a function that represents the volume fraction of cement gel produced by early-age chemical reactions and it depends on the total reaction degree and material parameters and Also, is the non-aging micro-compliance function of cement gel, with as the loading time interval and is another mesoscale model parameter that corresponds to the macroscale parameter in the original formulation, and the reduced time concept is introduced to account for the effect of change in relative humidity and temperature, where and , are the relative humidity and temperature (in Kelvin) at time t, R is the universal gas constant and is the activation energy for the creep processes.

The third component is the purely viscous strain rate which represents the unrecoverable part of the creep deformation and is given by , where S is the microprestress computed by solving the differential equation , and are model parameters, is a mesoscale model parameter that corresponds to the macroscale parameter in the original formulation, and . In this differential equation, the initial value at time is assumed to be a model parameter.

<Subhead 1>

Hygro-Thermo-Chemical (HTC) Model

To accurately simulate shrinkage and creep behavior of concrete, the values of temperature, , relative humidity, , and cement hydration degree, , must be defined both spatially and temporally over the simulated geometry. Without such presentation, key mesoscale mechanisms will not be correctly captured including cracks induced by inhomogenous shrinkage strains. In this regard, a comprehensive three-dimensional Hygro-thermo-Chemical (HTC) model for the evolution of temperature, humidity and cement hydration degree is utilized [14] as a Semi-Discrete Multi-Physics (SDMP) model. Based on this model, and distributions can be computed by imposing moisture mass

balance and enthalpy balance equations in the volume of interest. For temperature not exceeding C, moisture mass balance can be given by and enthalpy balance is given by. Cement hydration can be characterized by the hydration degree that represents the fraction of Portland clinker fully reacted with water. Its evolution law can be formulated as . The moisture permeability is described as , where , , and n are permeability constants, , where .

<Subhead 1>

Numerical implementation of various strain components

All strain rates described and formulated in the previous section are integrated in the LDPM framework. For each one, its three vectorial components at a generic facet connecting two aggregate pieces are integrated explicitly to compute its corresponding strain increments during the time step of the procedure to be fully explicit, all state variables (, , , and) are assumed to remain constant during the time step. Their values at the beginning of the time step are used to advance the solution in time. This is a fairly acceptable assumption provided that the time step used is small enough to guarantee stability and minimal integration errors.

In this study, all environmentally induced strains are treated as completely imposed strains, so it is only required to evaluate the LDPM strain rate at the beginning of each time step by rearranging of Eq. 1 in an incremental form as

Given the total facet strain rate $\dot{\varepsilon}$ at the beginning of each time step, the total strain increment is computed by . Then, all imposed strain increments are subtracted from to compute the concrete skeleton strain increment , which is used by the LDPM constitutive law to compute the corresponding facet stress vector increment and update the stress vector at the end of the time step.

Shrinkage and thermal strain increments are computed at the beginning of the time step as and

Creep strain is formulated at the facet level using the assumption of constant stress in the

time step increment as stated earlier. The viscoelastic creep strain is modeled as an aging multi Kelvin chain model. For a one-dimensional single Kelvin model with spring constant and damper coefficient the stress given by , where is the strain. Let be the system time constant. For the time step from to with , the stress is considered constant as . The strain increment for a chain of Kelvin elements at time is given by [24]. The non-aging compliance is computed for each chain to satisfy . Ten chains are used ranging from to days. This gives for [25]. With these values for, where is computed based on an approximate retardation spectrum of order 3 [24]. Also by considering a constant over the time step, one can write, . So, including all effects, the viscoelastic strain increment becomes . The purely viscous strain increment at the facet level is and the microprestress update is .

<Subhead 1>

Relaxation model

The relaxation model used is based on Eurocode 2 model [15], where the reduction in stress due to relaxation is evaluated as Δ, where and are constants based on class of steel, is initial post-tensioning, or pre-tensioning after immediate losses, pre-stress applied, the precept value of relaxation loss at 1000 hours after tensioning, is characteristic tensile strength of the prestressing steel, and t is time (in hours), after prestressing,

Initial prestressing and change in prestressing due to relaxation are imposed to two node elements, modeling steel tendons, as an eign-strain. The stain is based on bi-linear elasto-plastic constitutive relation for prestressing steel. This allows the interaction between this model, and other models such as creep, shrinkage, and concrete-rebar interaction through the total sum of strains.

Numerical Simulations

In order to validate the proposed models, simulations of a comprehensive experimental set [2] were performed. The mix design of used concrete was: water/cement ration of 0.5, aggregate/cement ration of 5.4, cement content of 340 kg/m^3, and maximum aggregate

size of 10 mm.

Companion cylinders (76mmX267mm) were used to determine concrete compressive strength and modulus of elasticity at different ages. Similarly, after 8 days of curing, two sets of cylinders were differently conditioned. The first was kept in either 99% relative humidity and the second was kept in 65% relative humidity both at . For both sets, shrinkage and creep strains were measures under no load and a uniaxial compressive stress of 5 MPa respectively.

The prestressed concrete beams had a rectangular cross section of (100mmX180mm), with an effective length of 2600 mm. The beams were post tensioned using a non-grouted 7 mm straight wire running in 15 mm duct at 50 mm from the bottom. After 8 days of curing (including casting day), Beams were prestressed with 48.3 KN and exposed to 65% relative humidity at , then loaded in a 3 Point Bending set up with 4 KN after one day of prestressing.

<Subhead 1>

Calibration of LDPM parameters

The calibration of LPDM parameters was based on compressive strength of 41.4 MPa and modulus of elasticity of 34.8 GPa at 28 days for concrete. The mesoscale tensile strength was estimated suing ACI 318-16 [27] splitting strength of MPa. Assuming Poisson ratio of 0.176, which gives , the meso-scale elastic modulus could be calculated as GPa. The initial fracture energy, could be estimated as N/m [26], where is the maximum aggregate size. Meso-scale fracture energy could be assumed equal to the initial fracture energy, and the meso-scale tensile characteristic length could be computed as mm [9, 28]. Finally, was calibrated to be 3.2, by simulating the reported compressive strength tests. The model generated for these simulations was a cylinder of the same dimensions as experimental ones, utilizing a fine mesh with minimum aggregate size of 5 mm, as shown in figure 2a. Figure 3 shows the evolution of relative humidity gradient with time, based on calibrated parameters, for 65% RH case.

<Subhead 1>

Calibration of HTC parameters

The calibration of HTC parameters was based on the swelling and shrinkage strains of cylinders put in 99% and 65% RH respectively, after 8 days of casting. Based on an estimated shrinkage coefficient of 2.15e-3, moisture permeability coefficients (,), and n were calibrated as (2.0e-10, 4.9e-7) , and 3.5 respectively to match the swelling/shrinkage evolution, then refined by the hydration parameters , , and as 15.0e6 , 1.0e-4, and 5.0 respectively. Figure 3 shows the matching between experimental data and calibrated model. Similar to LPDM section, simulations were performed on the fine mesh.

<Subhead 1>

Calibration of creep parameters

The calibration of creep parameters was performed on the same cylindrical geometries used in the previous section, but loaded at sustained stress of 5 MPa after 8 days. Based on basic and drying creep evolutions from the experimental data, creep compliance parameters (, ,) were calibrated as (0.75e-5, 1.25 e-5, 1e-6) and of 6.0e-3 . Figure 3 shows the matching in compliance between calibrated model for cylinders and experimental data. Similar to LPDM section, simulations were performed on the fine mesh.

<Subhead 1>

Coarse graining

A major challenge with modeling full-scale specimens is the computational cost needed by such comprehensive models. If the actual aggregate size was used, the beam specimen would have had 100887 nodes and 605322 Degrees of freedom. With a coarser mesh for the beam, as will be discussed later, using 15 mm as minimum aggregate size and 5234 nodes, the simulation s were performed on 64 parallel processors for 6 hours. As the solver used is an explicit solver, computational time scales proportionally with the number of nodes. This means that the fine mesh for the full-scale beam would need about 120 hours to run using the same number of processors, or would need 1235 processors to

run for the same time. Thus, the use of multi-scaling techniques is considered an effective solution for this problem. The authors successfully used coarse graining [22] to simulate bending and shear failure of plain and reinforced concrete beams and shear walls. Thus, the same coarse graining technique was used here. A scaling factor of 3 was used to coarsen the aggregate (thus reducing the number of degrees of freedom). Beam geometries with minimum aggregate size of 15 mm were generated and used for simulations. As reported in [22], elastic behavior is not affected by small scaling as long as the geometry is not under sampled (i.e. enough aggregate population is presented). As the stresses on the beam were in order of 5 MPa, very limited effects were expected. To check this assumption, cylinders were modeled with the coarse mesh, as shown in figure 2b, and results were compared with the fine mesh.

<Subhead 1>

Simulations of prestressed beams

A rectangular post-tensioned non-grouted beam was modeled using the calibrated LDPM and HTC parameters from cylinders data. The environmental change in boundary and mechanical loading was performed at multiple stages: 1) the beam was exposed to 99% RH, then dropped to 65% RH after 8 days, 2) gravitational forces were applied to count for mounting of the beam on the loading frame, 3) the prestressing force (43.8 KN) was applied to the stand, with assumed , finally 4) 4 KN was applied after one day and sustained with time. Coarse graining was used, generating a coarser mesh with a minimum aggregate size of 15 mm. Figure 4 shows the coarse aggregate mesh for the concrete beam, supporting and loading plates, steel cages, and prestressing wire. Supporting and loading plates, and steel cages were modeled using elastic steel model, while the relaxation model was used to represent constitutive relation of steel wire.

Results and discussion

The prediction of full-scale beam behavior followed series of independent calibration steps on small-scale companion specimens.

First, LPDM parameters were calibrated to match the reported strength and modulus of

elasticity. Second, HTC parameters were calibrated, as shown in figure 3, in order to match shrinkage and swelling of cylinders. It is important to note that the uniqueness of calibration is dependent on independency in experimental data. For example, having shrinkage profiles at different relative humidity boundary conditions insures the accurate estimation for shrinkage coefficient and diffusion parameters. Figure 5 shows the evolution of shrinkage stain with time, after 8 days of casting. Starting from this point till about 14 days, there is good matching between experimental and numerical results. After that, the model has higher shrinkage and lower swelling values. This could be relied to scatter in experimental data and the numerical high order terms error while solving and interpolation.

Third, Creep parameters were calibrated, as shown in figures 6, to match basic and drying creep of cylinders, starting from loading point at 8 days. Creep compliance from numerical data shows good matching up to 100 days, then it started to deviate. This could be relied to scatter in experimental data and the fact the experimental creep measurements are the difference between uniform loaded strains at the middle and surface shrinkage strains.

the use of coarse graining allowed for the simulation of large scale structural elements with a reasonable computational cost and without significant effects on accuracy, as shown in figure 4 and 5.

Fourth, as shown in figures 7 and 8, both shrinkage and creep strains are for coarse mesh had marginal differences from the fine mesh. These differences are within the experimental scatter known for concrete testing.

Finally, a strong validation of the procedure was through the prediction of the full-scale beam behavior. Figure 9 shows the predicted evolution of RH with time inside the center of beam the beam. It starts with full saturation, then humidity drops at the boundaries to 65%. As the beam section is larger than cylinders, the diffusion of water in lower than the cylinder as expected. While RH is about 74% and 65% after 400 and 100 days for the cylinders, it is about 85% and 72% at the same points of time. Figure 6 shows the predicted deflections for the beam. The solid line represents the average of the numerical

simulations and the grey area shows a range. In figure 6a, the total deflection is compared to measured deflection, starting from casting. The model predicts with good accuracy the upward camber at 8 days of -1 mm, then net deflection due to loading at 9 days of 0.1 mm.

To illustrate long-term behavior, figure 6b shows only deflection due to loading, starting from 9 days. As can be seen, the model was able to accurately predict instantaneous deflections after loading. It has to be also noticed that the figure is drawn in logarithmic time scale, which means that the model predictions of long-term deformation are quite accurate as the modeled response follows the experimental trend and does not plateau. Additionally, the reported measurements were experimental averages and as it is well known for these types of experiments, a noticeable scatter is usually reported. Finally, a limitation of the framework can be attributed to the phenomenological nature of the relaxation formulation, which is planned to be the point of future consideration of the researchers, and other types of prestressing losses that were not counted for.

Conclusion

In this paper, a multi-scale multi-physics framework was presented to model prestressed concrete beams. Model parameters were calibrated using companion specimens, for LDPM, HTC, shrinkage, and creep models then used to predict the behavior of full-scale beams. An exponential model was adopted to present the effect of steel relaxation. Predicted beam behavior matched the upward camber, instantaneous deflection due to loading, and followed the same trend for long-term behavior within an experimentally acceptable error margin. A more refined model for relaxation is to be developed by the authors in the future to better match actual responses.

Acknowledgment

The authors would like to acknowledge the support from the Rensselaer Polytechnic Institute Center for Computational Innovations (CCI) to run the simulations in this paper using the High performance computing clusters at both centers.

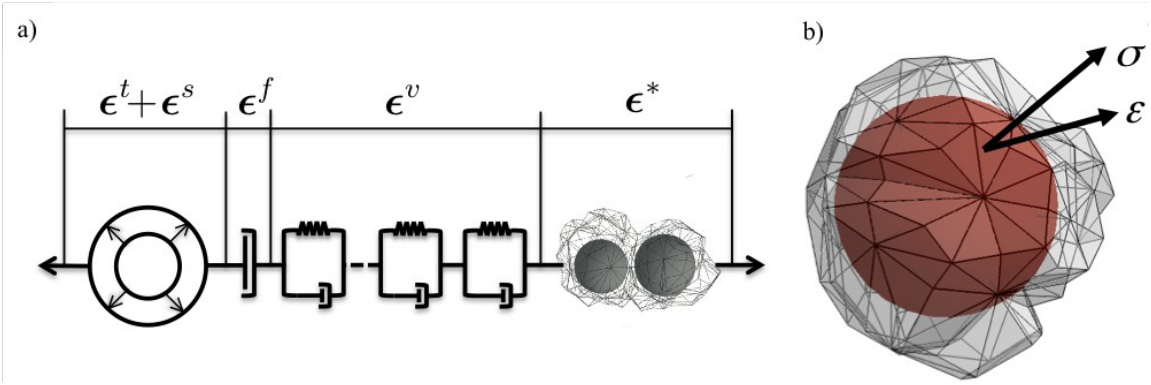

Figure 1: a) Equivalent rheological model based on strain additively, b) One LDPM Cell around an aggregate piece with facet stress and strain vector

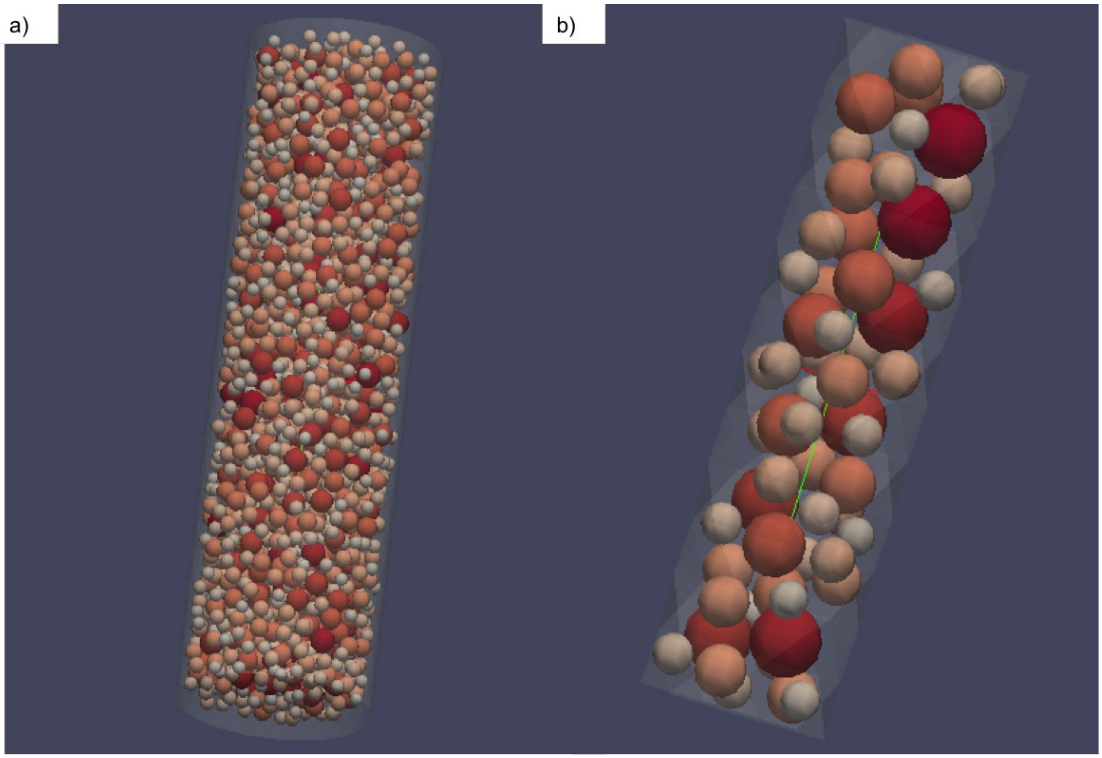

Figure 2: a) Fine LPDM mesh with minimum aggregate size of 5 mm, b) Coarse LPDM mesh with minimum aggregate size of 15 mm

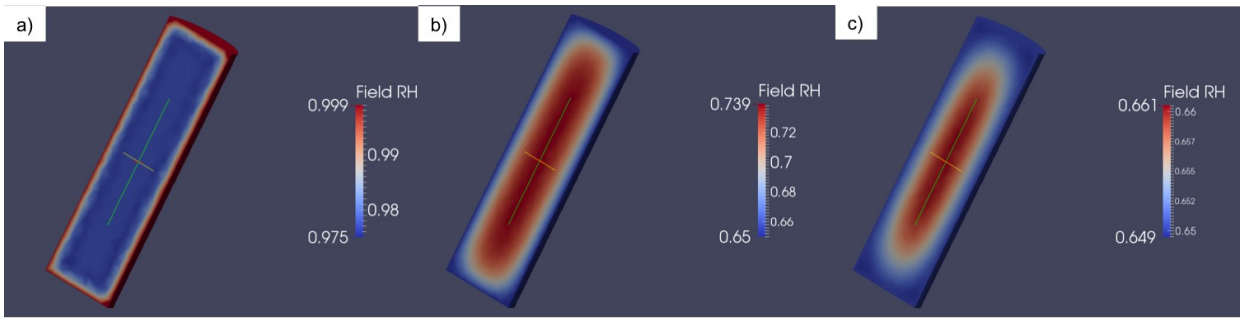

Figure 3: The evolution of RH gradient with time for 65% cylinders at: a) 2 days, b) 100 days, and c) 400 days.

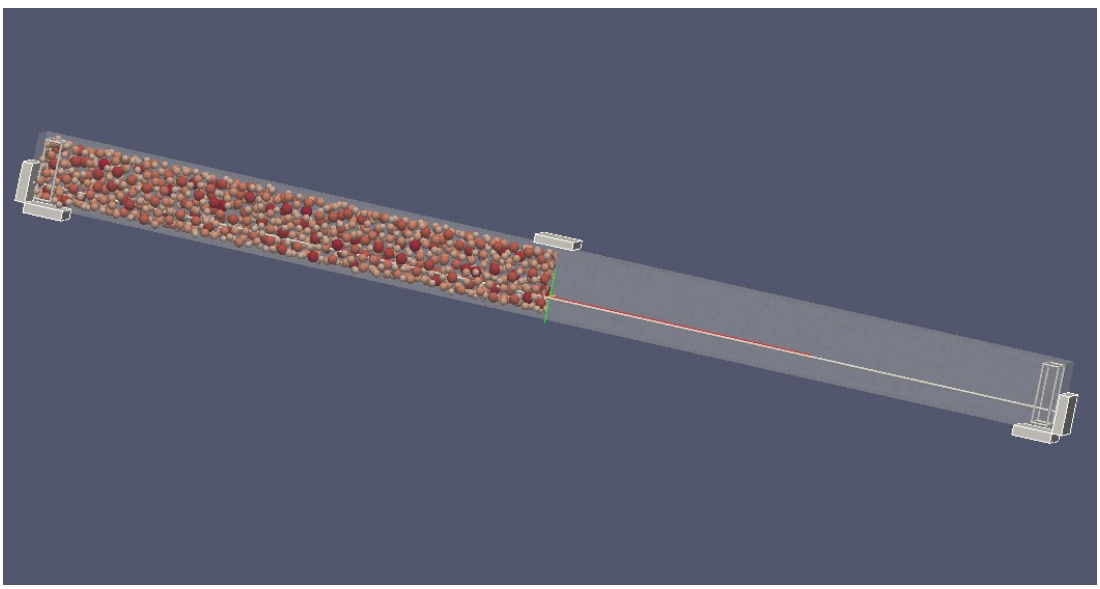

Figure 4: Coarse LPDM mesh for full-scale beam.

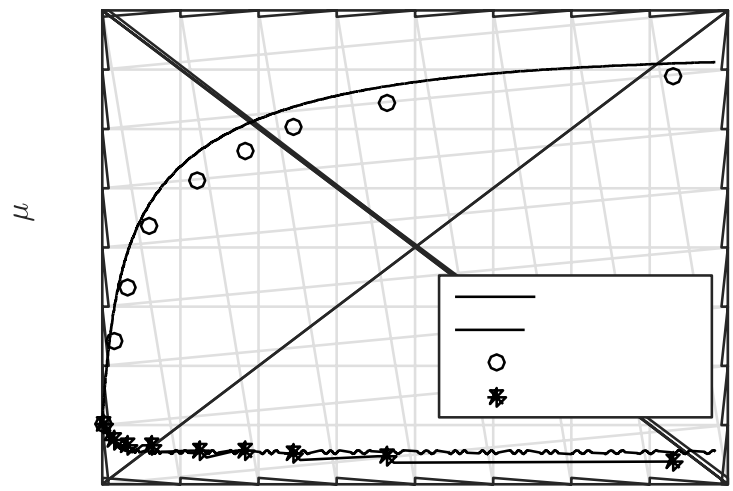

Figure 5: Shrinkage and swelling strains for cylinders, after 8 days of casting.

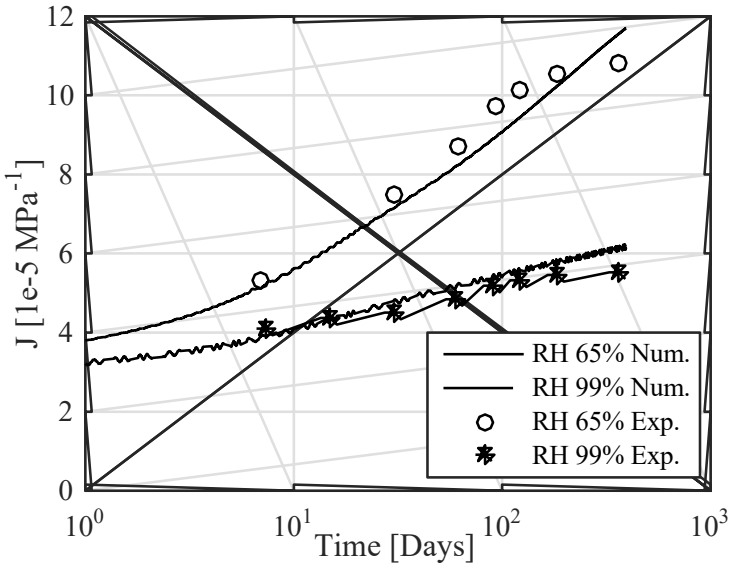

Figure 6: Basic and drying creep compliance for cylinders, after 8 days of casting.

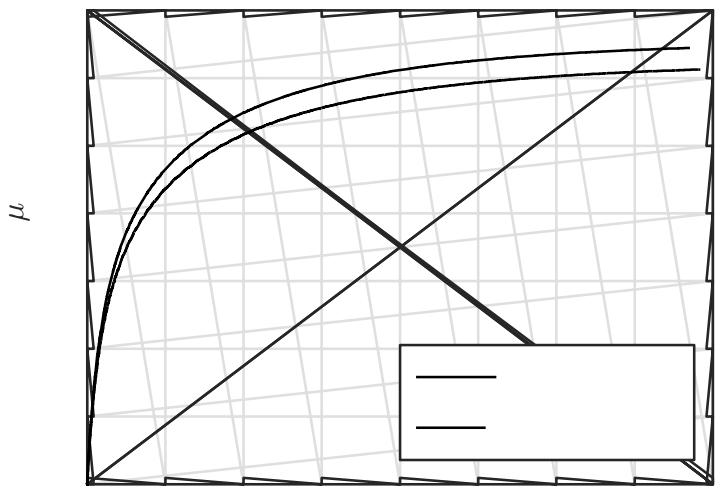

Figure 7: Comparison of fine and coarse shrinkage strains for cylinders.

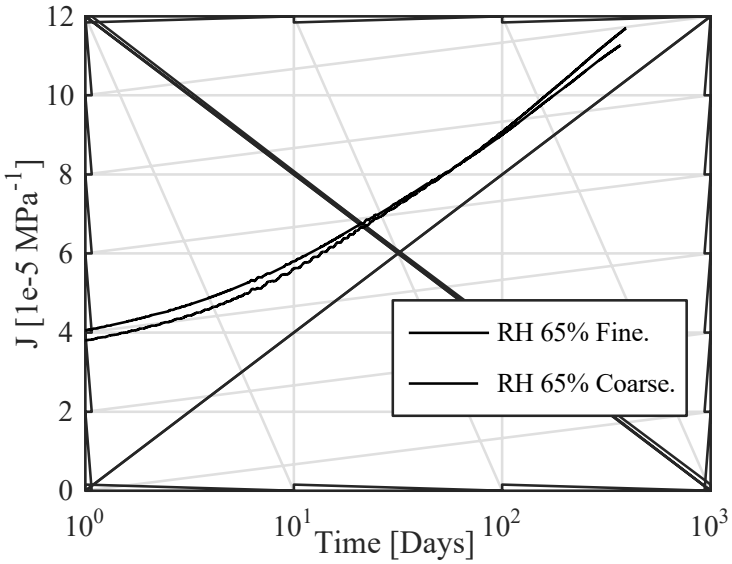

Figure 8: Comparison of fine and coarse drying creep compliance for cylinders.

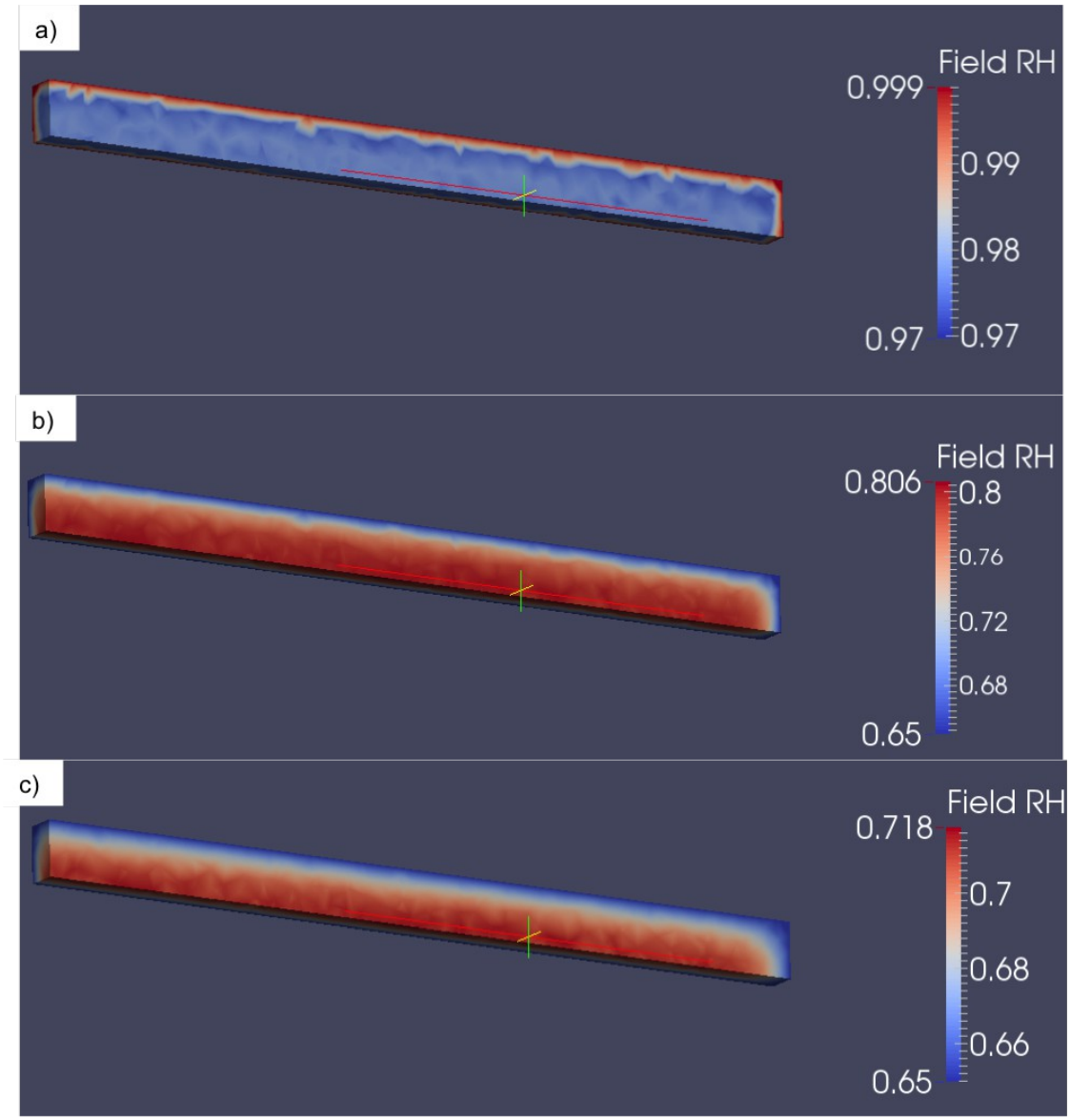

Figure 9: The evolution of RH gradient with time inside full-scale beam at: a) 2 days, b) 100 days, and c) 400 days.

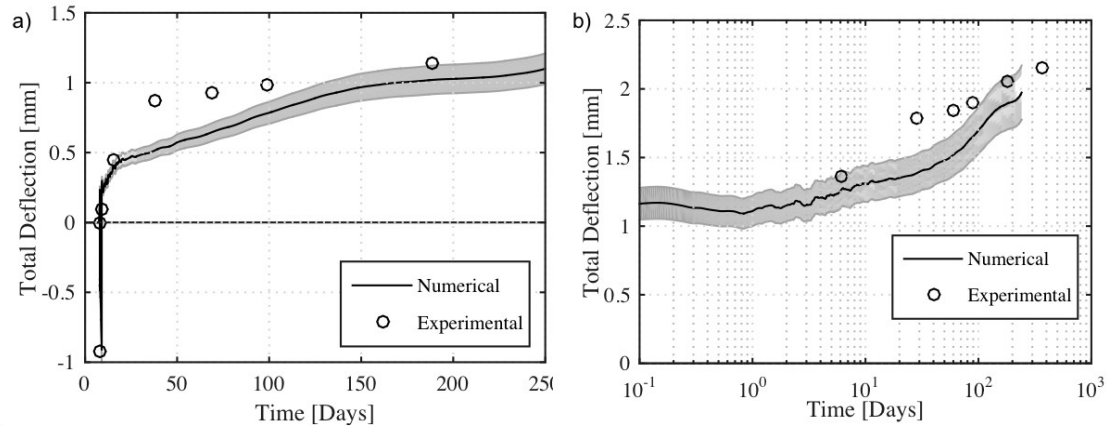

Figure 10: a) Total beam deflection from casting, b) long term beam deflection measured from loading.

References

[1] Bazant, Z. P., Yu, Q., Li, G. H., Klein, G. J., & Kristek, V. (2010). "Excessive deflections of record-span prestressed box girder." Concrete International, 32(06), 44-52.

[2] Al-Khaja, W. A. A. (1986). "Time-dependent losses in post-tensioned prestressed concrete." Doctoral dissertation, University of Leeds.

[3] Asamoto, S., Kato, K., & Maki, T. (2014). "Effect of creep induction at an early age on subsequent prestress loss and structural response of prestressed concrete beam." Construction and Building Materials, 70, 158-164.

[4] Magura, D. D., Sozen, M. A., & Siess, C. P. (1963). "A study of stress relaxation in prestressing reinforcement." University of Illinois.

[5] Kwak, H. G., & Seo, Y. J. (2002). "Numerical analysis of time-dependent behavior of pre-cast pre-stressed concrete girder bridges." Construction and building materials, 16(1), 49-63.

[6] Lou, T., Lopes, S. M., & Lopes, A. V. (2013). "Nonlinear and time-dependent analysis of continuous unbonded prestressed concrete beams." Computers &

Structures, 119, 166-176.

[7] Lou, T., Lopes, S. M., & Lopes, A. V. (2014). “A finite element model to simulate long-term behavior of prestressed concrete girders.” Finite Elements in Analysis and Design, 81, 48-56.

[8] Cusatis, G., Mencarelli, A., Pelessone, D., and Baylot, J. (2011a). “Lattice discrete particle model (ldpm) for failure behavior of concrete. II: Calibration and validation.” Cement and Concrete Composites, 33(9), 891–905.

[9] Cusatis, G., Pelessone, D., and Mencarelli, A. (2011b). “Lattice discrete particle model (ldpm) for concrete failure behavior of concrete. I: Theory.” Cement and Concrete Composites, 33(9), 881–890.

[10] Abdellatef, M., Alnaggar, M., Boumakis, G., Cusatis, G., Di-Luzio, G., and Wendner, R. (2015) “Lattice Discrete Particle Modeling for Coupled Concrete Creep and Shrinkage Using the Solidification Microprestress Theory.” CONCREEP 10: pp. 184-193.

[11] Di-Luzio, G. and Cusatis, G. (2013). “Solidification–microprestress–microplane (smm) theory for concrete at early age: Theory, validation and application.” International Journal of Solids and Structures, 50, 957–975.

[12] Bazant, Z. P., Hauggaard, A. B., Baweja, S., and Ulm, F.-J. (1997). “Microprestress-solidification theory for concrete creep. I: Aging and drying effects.” Journal of Engineering Mechanics, 123(11), 1188–1194.

[13] Bazant, Z. P., & Prasannan, S. (1989). Solidification theory for concrete creep. I: Formulation. Journal of engineering mechanics, 115(8), 1691-1703.

[14] Di-Luzio, G. and Cusatis, G. (2009a). “Hygro-thermo-chemical modeling of high performance concrete. I: Theory.” Cement and Concrete Composites, 31(5), 301–308.

[15] British Standards Institution. (2004). Eurocode 2: Design of Concrete Structures: Part 1-1: General Rules and Rules for Buildings. British Standards Institution.

[16] Schauffert, E. A. and Cusatis, G. (2012). “Lattice discrete particle model for fiber reinforced concrete (ldpm-f): I. theory.” Journal of Engineering Mechanics, 138(7), 826–833.

[17] Smith, J., Cusatis, G., Pelessone, D., Landis, E., O’Daniel, J., and Baylot, J. (2014). “Discrete modeling of ultra-high-performance concrete with application to projectile penetration.” International Journal of Impact Engineering, 65, 13–32.

[18] Alnaggar, M., Cusatis, G., and Di-Luzio, G. (2013). “Lattice discrete particle modeling (ldpm) of alkali silica reaction (asr) deterioration of concrete structures.” Cement and Concrete Composites, 41, 45–59.

[19] Alnaggar, M., Cusatis, G., Qu, J., & Liu, M. (2013). “Simulating acoustic nonlinearity change in accelerated mortar bar tests: A discrete meso-scale approach.” Innovation, Communication and Engineering, 1, 451.

[20] Alnaggar, M. (2014). “Multiscale modeling of aging and deterioration of reinforced concrete structures.” Ph.D. thesis, Northwestern University, Northwestern University.

[21] Abdellatef, M., Salem. S. , Lau, D., Stenroos, L., and Alnaggar, M. (2016) “Lattice Discrete Particle Modeling for Coupled Concrete Creep and Shrinkage Using the Solidification Microprestress Theory.” FraMCoS-9.

[22] Alnaggar, M. and Cusatis, G. (2012). “Automatic parameter identification of discrete mesoscale models with application to the coarse-grained simulation of reinforced concrete structures.” ASCE 2012 Structures Congress, 36, 406–417.

[23] Cusatis, G., Rezakhani, R., Alnaggar, M., Zhou, X., and Pelessone, D. (2014). “Multi- scale computational models for the simulation of concrete materials and structures.” CRC Press, 23–38.

[24] Bazant, Z. P. and Xi, Y. (1995). “Continuous retardation spectrum for solidification theory of concrete creep.” Journal of Engineering Mechanics, 121, 281–288.

[25] Bazant, Z.P., Cusatis, G., and Cedolin, L. (2004). “Temperature effect on concrete

creep modeled by microprestress-solidification theory." Journal of Engineering Mechanics, 130(Special Issue: Constitutive Modeling of Geomaterials), 691–699.

[26] Bažant, Z. P., & Becq-Giraudon, E. (2002). "Statistical prediction of fracture parameters of concrete and implications for choice of testing standard." Cement and Concrete Research, 32(4), 529-556.

[27] ACI Committee, American Concrete Institute, and International Organization for Standardization. "Building code requirements for structural concrete (ACI 318-16) and commentary." American Concrete Institute, 2016.

[28] Cusatis, G., & Cedolin, L. (2007). Two-scale study of concrete fracturing behavior. Engineering Fracture Mechanics, 74(1), 3-17.